AJR American Journal of Roentgenology

Applications of Artificial Intelligence for Pediatric Cancer Imaging

Shashi B. Singh, MBBS[1], Amir H. Sarrami, MD[1], Sergios Gatidis, MD[1], Zahra S. Varniab, MD[1], Akshay Chaudhari, PhD[2,3], Heike E. Daldrup-Link, MD, PhD[1,4]

Pediatric Imaging · Review

Keywords

artificial intelligence, cancer, machine learning, pediatrics, radiology

Submitted: Feb 25, 2024
Revision requested: Mar 8, 2024
Revision received: Apr 19, 2024
Accepted: May 21, 2024
First published online: May 29, 2024
Version of record: Aug 14, 2024

The authors declare that there are no disclosures relevant to the subject matter of this article.

Supported in part by a stipend from the Stanford Center for Artificial Intelligence in Medicine & Imaging (AIMI) and the Human-Centered Artificial Intelligence (HAI) Program at Stanford University (to S.B.S. and A.H.S.). The research projects of the authors, described and cited in this article, were supported by the National Cancer Institute (grant R01CA269231).

Artificial intelligence (AI) is transforming the medical imaging of adult patients. However, its utilization in pediatric oncology imaging remains constrained, in part due to the inherent scarcity of data associated with childhood cancers. Pediatric cancers are rare, and imaging technologies are evolving rapidly, leading to insufficient data of a particular type to effectively train these algorithms. The small market size of pediatric patients compared with adult patients could also contribute to this challenge, as market size is a driver of commercialization. This review provides an overview of the current state of AI applications for pediatric cancer imaging, including applications for medical image acquisition, processing, reconstruction, segmentation, diagnosis, staging, and treatment response monitoring. Although current developments are promising, impediments due to the diverse anatomies of growing children and nonstandardized imaging protocols have led to limited clinical translation thus far. Opportunities include leveraging reconstruction algorithms to achieve accelerated low-dose imaging and automating the generation of metric-based staging and treatment monitoring scores. Transfer learning of adult-based AI models to pediatric cancers, multiinstitutional data sharing, and ethical data privacy practices for pediatric patients with rare cancers will be keys to unlocking the full potential of AI for clinical translation and improving outcomes for these young patients.

Artificial intelligence (AI) algorithms are transforming the medical imaging of adult patients, facilitating image acquisition, reconstruction, quality control, segmentation, analysis, and interpretation [1–6]. However, the development of AI algorithms for pediatric applications and, in particular, for pediatric oncologic applications is limited to date. According to an overview by the American College of Radiology, only 3% of FDA-approved AI applications for medical image analysis (seven of 221 total products) are tailored for pediatric imaging [7]. None of these are specific to oncologic applications in children, highlighting a critical gap in addressing the diagnosis and treatment of pediatric cancer with AI-powered tools.

Algorithms approved for adult patients can potentially be used in children, with the likelihood of success strongest if the imaging technique and anatomy are similar in children and adults for the given context. However, to date, limited evidence has addressed the performance of adult algorithms when applied in children. One example that has been explored is the use of AI algorithms for automated lung nodule detection on chest CT [8]. However, studies have found that adult-based lung nodule detection algorithms do not perform as well in children as they do in adults [8, 9].

Many AI algorithms for pediatric cancer applications require specific development for children. However, the rarity of childhood cancers and the ongoing rapid evolution of imaging technologies limit the availability of large standardized datasets, which in turn hinders robust training of AI models for pediatric oncology applications. The rarity of childhood cancers translates to a smaller patient population; as market size is a driver of commercialization, this smaller market size of pediatric patients compared with adult pa-

ARRS is accredited by the Accreditation Council for Continuing Medical Education (ACCME) to provide continuing medical education activities for physicians.
The ARRS designates this journal-based CME activity for a maximum of 1.00 AMA PRA Category 1 Credit™. Physicians should claim only the credit commensurate with the extent of their participation in the activity.
Use the "Claim Credit" link to access the CME activity.

doi.org/10.2214/AJR.24.31076
AJR 2024; 223:e2431076
ISSN-L 0361-803X/24/2232–e2431076

[1]Department of Radiology, Division of Pediatric Radiology, Stanford University School of Medicine, 1201 Welch Rd, Stanford, CA 94305. **Address correspondence to** H. E. Daldrup-Link (heiked@stanford.edu, @PedsMIPS).

[2]Department of Radiology, Integrative Biomedical Imaging Informatics (IBIIS), Stanford University School of Medicine, Stanford University, Stanford, CA.

[3]Department of Biomedical Data Science, Stanford University School of Medicine, Stanford University, Stanford, CA.

[4]Department of Pediatrics, Pediatric Hematology-Oncology, Lucile Packard Children's Hospital, Stanford University, Stanford, CA.

tients potentially and, in association with relatively limited financial returns, could be a disincentive to developers. Another major challenge is the lack of publicly available whole-body image datasets of children with cancer. Of 208 imaging datasets published (as of March 19, 2024) on The Cancer Imaging Archive, one of the largest public cancer imaging databases, eight are dedicated pediatric datasets [10]. The Cancer Imaging Archive collaboration with the Childhood Cancer Data Initiative of the National Cancer Institute provides a repository of high-quality CT, MR, and PET images of pediatric nasopharyngeal cancer, Hodgkin lymphoma, Wilms tumor, medulloblastoma or primitive neuroectodermal tumor, and liver cancer [10]. Another public imaging repository, the Medical Imaging and Data Resource Center, is continuously growing but does not have a dedicated pediatric oncologic context at this time [11]. The 2017 Radiological Society of North America (RSNA) database contains a large dataset of pediatric hand radiographs, which could be used as normal reference data [12]. The Children's Oncology Group has a central image registry Quality Assurance Review Center (QARC) of imaging studies of children with cancer before and after chemotherapy. The QARC image registry includes large but heterogeneous image datasets and can be accessed by interested parties through an administrative application process [13].

Many of these image registries include image datasets collected from different centers and scanners. The resulting advantage is that the registries provide data from patients with diverse demographic backgrounds. However, the heterogeneous imaging protocols and techniques of multiinstitutional image registries pose a challenge for training AI algorithms. The Children's Brain Tumor Network (CBTN) addressed this problem by generating consensus about a shared imaging protocol before collecting image data for 4900 patients in a shared database [14]. Similar efforts initiated by the Children's Oncology Group or other authoritative bodies could enhance the utility of their image registries for AI algorithm development.

Although the field of AI development is rapidly expanding, the impact of AI algorithms on the care of children with cancer has not yet been established. Today, most AI systems primarily focus on slice-by-slice or single-plane image analysis. However, imaging studies of children with cancer often require multiplanar or volumetric analysis, which are beyond the capabilities of current AI solutions. AI struggles with complex anatomic structures and pathologies spanning multiple imaging planes. Although AI holds immense promise, real-world gains have been relatively slow.

This review provides an overview of the current state of AI applications for pediatric cancer imaging, including applications for medical image acquisition, processing, reconstruction, segmentation, diagnosis, staging, and treatment response monitoring. Although some of the aspects of image data processing discussed can be applied to pediatric imaging in general, the downstream tasks related to tumor diagnoses are specific to oncologic imaging.

Image Data Acquisition and Processing

AI algorithms can be developed for upstream image processing (i.e., generation of medical images before interpretation) and downstream image processing (i.e., detection and characterization of areas of interest on a medical image). AI can enable safer image acquisition by reducing the patient's radiation exposure. Examples include augmenting low-radiotracer-dose PET images to standard-dose PET images [1, 3] and augmenting ultralow-dose CT images to standard-dose CT images [15]. AI can also accelerate imaging times by augmenting ultrafast low-resolution MR images to high-resolution images [16], enhancing image quality, and minimizing image noise. Some of these MRI augmentation algorithms are commercially available [17, 18]. However, most are trained on adult datasets and lack oncologic context.

Highlights

- *AI algorithms can accelerate the acquisition, reconstruction, and processing of medical images of pediatric cancers.*
- *Challenges in developing commercial AI algorithms for pediatric tumor segmentation include heterogeneous imaging protocols and patient anatomy, a paucity of multiinstitutional data, and limited market size.*
- *A critical gap exists between promising AI methods for pediatric cancer diagnosis and treatment response monitoring and their actual use in clinical practice.*

Chaudhari et al. [3] developed a deep learning algorithm for augmenting standard-dose PET images from fourfold reduced-count whole-body PET scans of children and young adult patients. Wang et al. [1] developed a novel AI model for the augmentation of ultralow-dose FDG PET/MR images of 33 children and young adults (age range, 3–30 years) with lymphoma, which reduced patients' radiation exposure by more than 90%. Next, Wang et al. [19] compared five AI models for enhancing the image quality of ultralow-dose pediatric PET scans. SwinIR and U-Net achieved superior performance compared with three other AI algorithms for augmenting ultralow-dose input images.

Many AI algorithms focus on pretreatment scans only and do not consider posttreatment scans. To address this gap, in 2021 Theruvath et al. [2] evaluated the performance of a convolutional neural network (CNN) for augmenting the static low-dose FDG PET/MRI scans of patients with pediatric lymphoma before and after chemotherapy. Simulated low-dose scans showed increased noise and decreased tumor-to-liver contrast, hindering therapy response assessment on posttreatment scans. Although CNN augmentation improved performance at 75% and 50% reduced-dose images, achieving sensitivity and specificity of 100% for response classification at both simulated doses, significant errors persisted if augmentation was attempted for images with simulated radiotracer dose reduction of more than 50% (i.e., simulated reductions of 25%, 12.5%, and 6.25%) [2] (Fig. 1).

Other than for PET, AI applications have also been studied to enhance image data acquisition and processing of MRI and CT. Ladefoged et al. [20] compared two MRI-based attenuation correction methods for PET/MRI scans of pediatric brain tumors. Both methods were as accurate as traditional CT-based attenuation correction. However, a DeepUTE algorithm outperformed Resolute (another MRI-based method). Maspero et al. [21] used MRI-derived synthetic CT (sCT) images for dose calculation in pediatric brain tumor radiotherapy. By combining sCT examinations

from multiple planes and accounting for MRI protocol variations, the method achieved accurate dose calculations with minimal discrepancies compared with standard CT. This finding supports MRI-based sCT as a promising tool for this application (Fig. 2).

A significant challenge in the application of AI for medical image augmentation lies in striking a careful balance between noise reduction and preservation of image fidelity [22]. Noise that can hinder analysis must be removed, while crucial details essential for accurate diagnosis simultaneously must be preserved. Image processing with AI algorithms can obscure subtle yet diagnostically relevant features. Despite the widespread adoption of AI-processed medical images, such as AI-processed single-shot T2-weighted or fast spin-echo (FSE) T2-weighted sequences, concern exists regarding the potential loss of crucial diagnostic information for AI-augmented MRI scans [23]. The original images can be accessed on some scanners. However, this process requires retrieving source images that may not be routinely provided on the PACS, adding a time-consuming step to the workflow.

AI algorithms for the augmentation of CT scans have been used to reduce the radiation exposure of children undergoing CT.

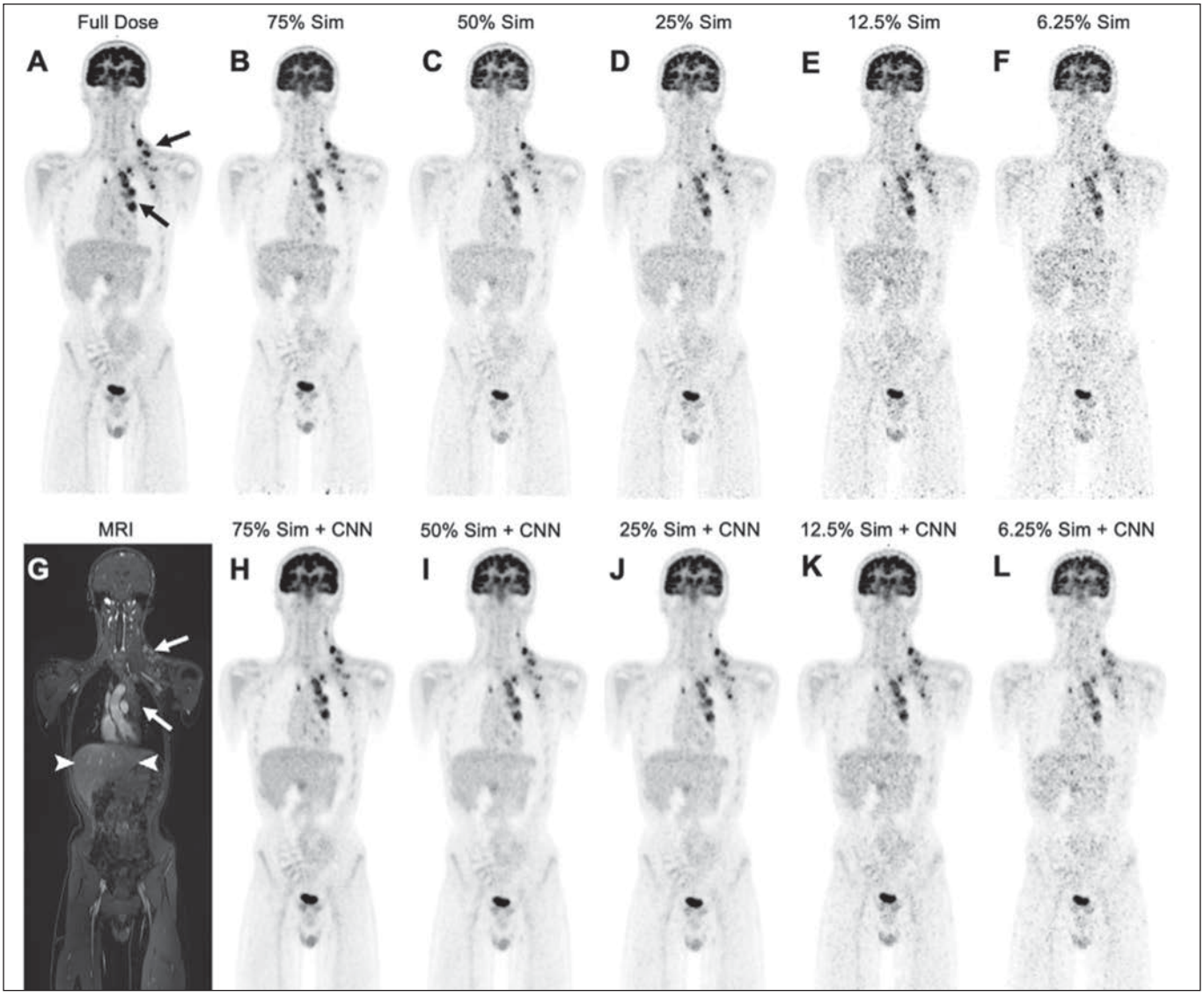

Fig. 1—14-year-old boy with Hodgkin lymphoma. (Used with permission of Radiological Society of North America, from Validation of deep learning-based augmentation for reduced ^{18}F-FDG dose for PET/MRI in children and young adults with lymphoma, Theruvath AJ, Siedek F, Yerneni K, et al. *Radiol Artif Intell*, 3, 2021; permission conveyed through Copyright Clearance Center, Inc.)
A, Hypermetabolic mediastinal and left infra- and supraclavicular lymph nodes (*arrows*) are clearly visible on full-dose FDG PET image (3 MBq/kg).
B–**F**, Increased noise and decreased tumor-to-liver contrast are seen on coronal FDG PET images obtained using simulated (Sim) reduced radiotracer doses of 75% (**B**), 50% (**C**), 25% (**D**), 12.5% (**E**), and 6.25% (**F**).
G, Increased noise and reduced contrast between tumor (*arrows*) and liver (*arrowheads*) are also seen on corresponding coronal MR image.
H–**L,** Corresponding low-dose FDG PET images augmented with convolutional neural network (CNN) show reduced noise and improved contrast between tumor and liver compared with non–CNN-augmented PET images.

Brady et al. [15] achieved a radiation dose reduction of 48% with the adaptive statistical iterative reconstruction algorithm (Fig. 3).

Salman et al. [24] assessed a commercially available lung computer-aided detection (CAD) system for pulmonary nodule detection on pediatric CT scans with simulated dose reductions (75%, 50%, and 25%). Sensitivity remained low (24–27%) but was not significantly impacted by lower doses.

Pediatric studies evaluating adult lung CAD algorithms on chest CT have reported concerning results. In a study by Salman et al. [8], a pediatric CAD system for lung nodule detection showed low sensitivity (26–39%) with moderate PPV (48–62%), even with thinner slices or exclusion of smaller nodules. These findings suggest that directly applying adult-derived algorithms to pediatric CT scans may not be effective, and they highlight the need for pediatric-specific AI development. A key hurdle in using existing AI models for pediatric data is the mismatch between training data and real-world applications. Models trained on adult data may underperform when encountering the distinct anatomies of children, potentially impacting diagnosis and treatment [25].

Image Segmentation

In medical imaging, segmentation involves the identification, localization, and isolation of predefined structure(s) within the medical image(s) to identify tumors, organs, or other structures for image processing and interpretation. Encoder-decoder architectures, such as the U-Net architecture [26, 27], have shown good overall performance in segmenting anatomic structures in adult patients, such as the abdominal organs [28, 29], cardio-

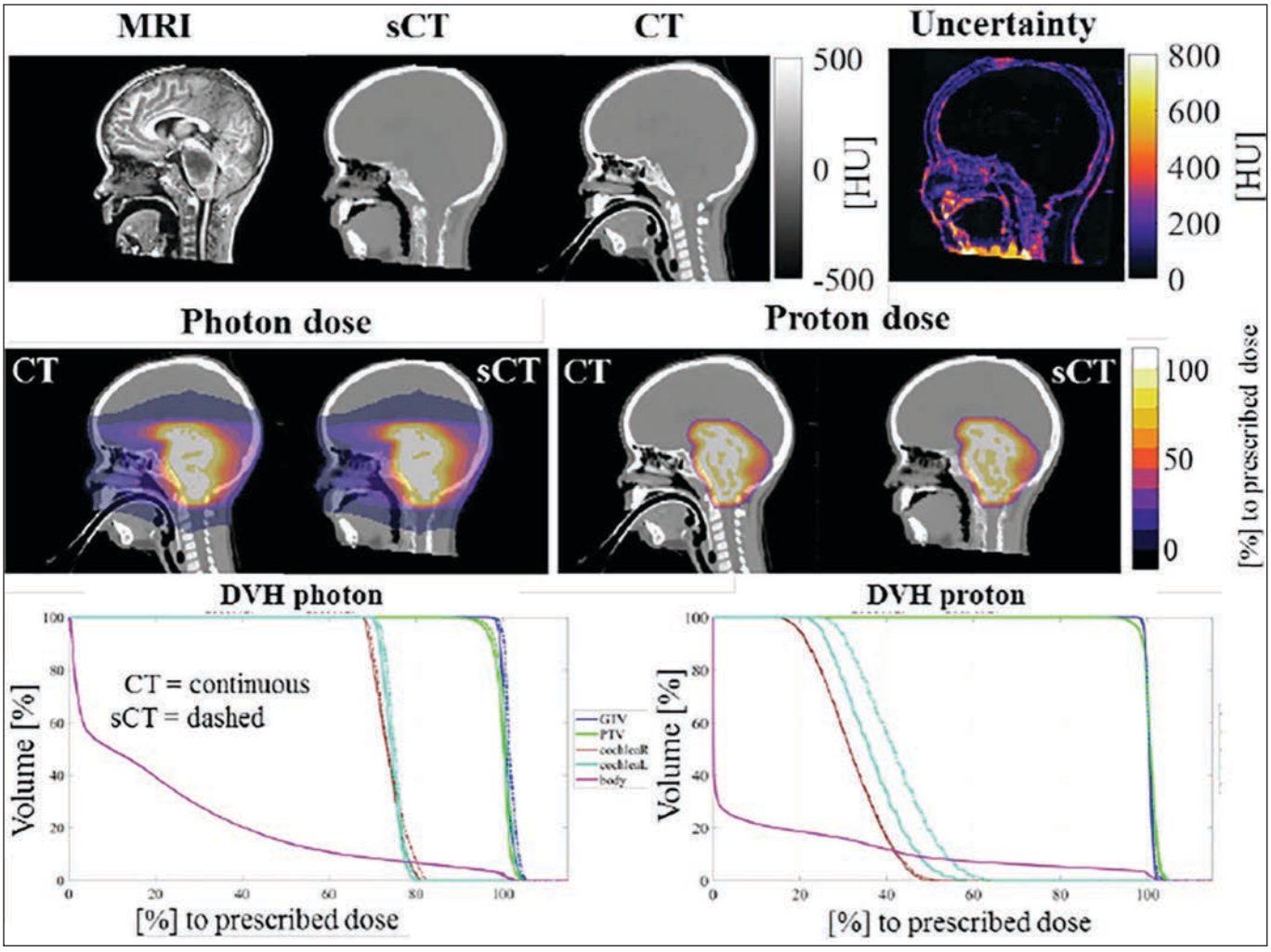

Fig. 2—5-year-old girl with diffuse intrinsic pontine glioma that was irradiated with palliative intent using prescribed dose of 39 Gy in 13 fractions. Top row (*left* to *right*) shows MR image, simulated CT (sCT) image, CT image, and uncertainty map. Middle row shows photon dose plan (*left*) and proton dose plan (*right*), as calculated on CT (*solid lines*) and sCT (*dashed lines*) as shown on respective dose-volume histograms (DVHs) (*bottom row*). MRI was acquired without gadolinium-based contrast media at 1.5 T. This patient had largest relative difference in photon dose in study sample, with difference of –0.8% for high-dose region (dose > 90% of prescription). MRI and CT were performed 3 days apart. Patient was scanned while under anesthesia, and tubes used for anesthetic administration are visible on both modalities. Quality of sCT is lower in neck region, toward end of MRI FOV; uncertainty is larger in same region. GIV = gross inner volume, PIV = planned inner volume, cochleoR = right cochlea, cochleoL = left cochlea. (Reproduced from Maspero M, Bentvelzen LG, Savenije MHF, Guerreiro F, Seravalli E, Janssens GO, van den Berg CAT, Philippens MEP. Deep learning-based synthetic CT generation for pediatric brain MR-only photon and proton radiotherapy. *Radiother Oncol* 2020; 153:197, © 2020, with permission under Creative Commons Attribution 4.0 International Public License [creativecommons.org/licenses/by/4.0/legalcode], including disclaimer of warranties in Section 5)

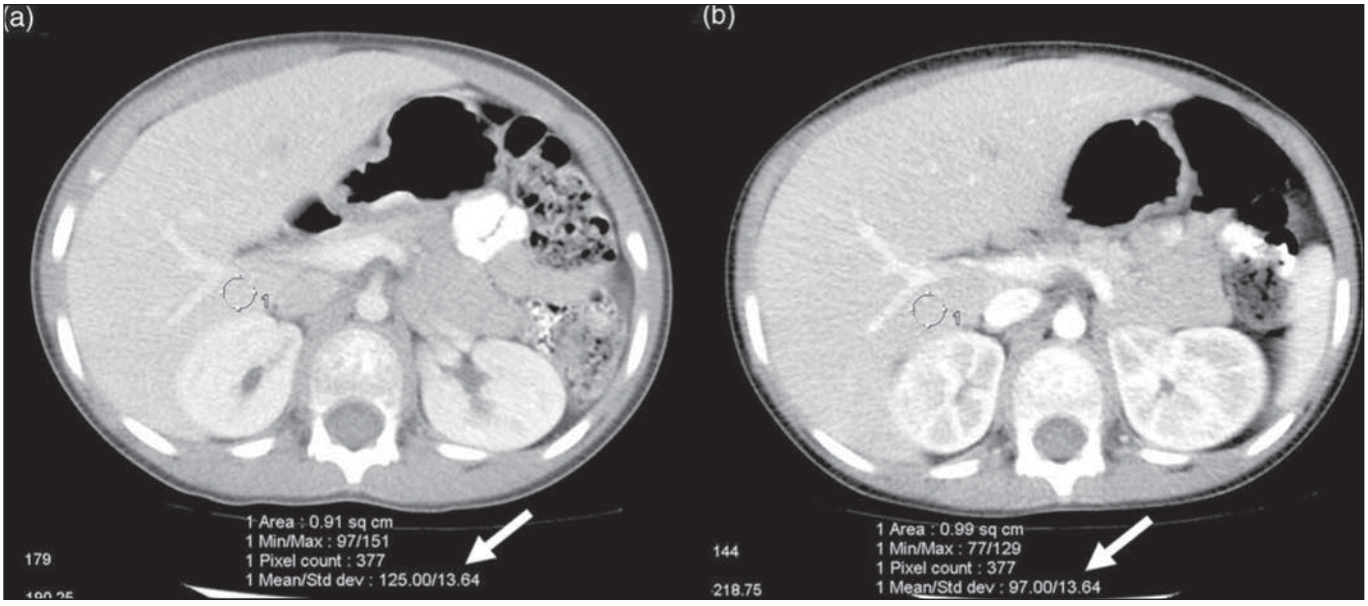

Fig. 3—Patient weighing 23 kg underwent two CT examinations performed approximately 30 days apart. Both images show same SD of attenuation of 13.64 HU (*arrow*) in 1-cm^2 ROI (*circle* labeled "1") posterior to right portal vein. Min = minimum, max = maximum, Std dev = SD. (Used with permission of John Wiley & Sons–Books, from Characterization of adaptive statistical iterative reconstruction algorithm for dose reduction in CT: pediatric oncology perspective, Brady SL, Yee BS, Kaufman RA, *Med Phys,* 39, 2012; permission conveyed through Copyright Clearance Center, Inc.)
A, Axial image from first CT examination, performed without adaptive statistical iterative reconstruction (ASiR).
B, Axial image from second CT examination, performed with ASiR at level of 40%. Use of ASiR increases noise index by 25% and reduces minimum milliampere-second for automatic tube current modulation. Second examination had dose reduction of 41%. ASiR is variant of model-based iterative reconstruction algorithm that uses advanced computational and statistical techniques integral to artificial intelligence.

vascular structures [29, 30], and neuroanatomy [29, 31]. However, there is a scarcity of segmentation algorithms for pediatric datasets. Recently, a small number of pediatric segmentation datasets have been published for automated CT-based segmentation of up to 29 anatomic organ structures per patient on 359 abdominopelvic CT examinations (with possible inclusion of the chest) [32], segmentation of six organ structures (liver, lungs, bladder, kidney, bones, and brain) on 140 CT images [33], and segmentation of the heart on 64 cardiac MR images [30].

Due to the relatively high standardization of brain MRI protocols, segmentation of brain tumors has been widely studied in adult and pediatric populations [31, 34–39]. The BraTS (Brain Tu-

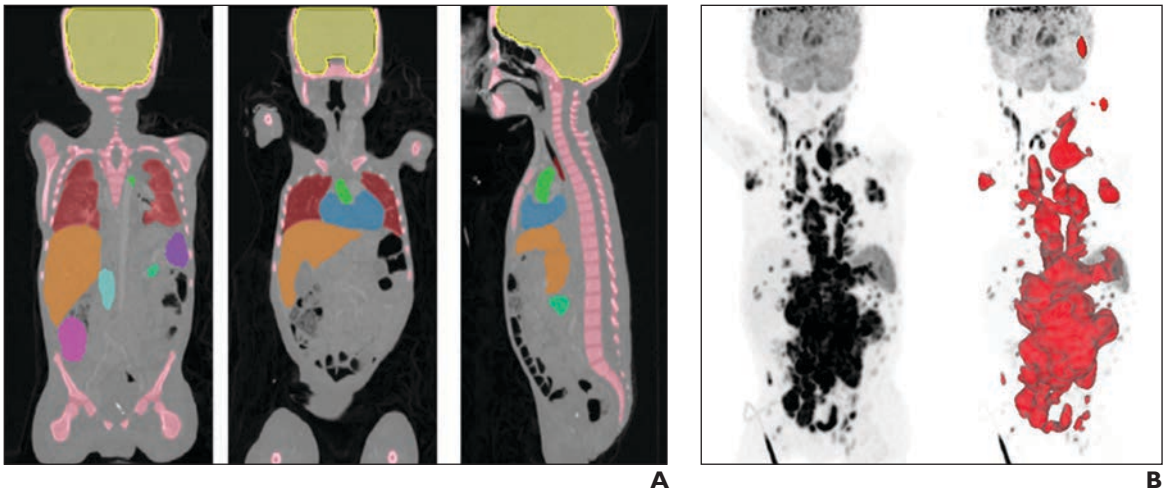

Fig. 4—5-year-old boy with posttransplant lymphoproliferative disorder (PTLD), evaluated by FDG PET/CT.
A, Coronal (*left* and *middle*) and sagittal (*right*) fused PET/CT images show automated multiorgan segmentation using publicly available U-Net deep learning model, including segmentation of brain (*yellow*), bones (*pink*), lungs (*red, left* and *middle*), trachea (*red, right*), heart (*blue*), aorta (*green*), liver (*orange*), and spleen (*purple*). Model was trained on adult population of patients with cancer [69].
B, Coronal PET images show automated segmentation of PTLD tumor lesions using available U-Net deep learning model. Model was trained in adult population of patients with lung cancer, lymphoma, and malignant melanoma [46].

mor Segmentation) [34] challenge was one of the first and most widely recognized biomedical machine learning challenges. Based on methodologic advances in brain tumor segmentation in adult populations, studies have recently described automated segmentation of pediatric brain tumors (glioma, ependymoma, and medulloblastoma) in MRI and PET/MRI data using deep learning techniques [35, 40].

Fully automated AI algorithms for the detection of pulmonary nodules on chest CT require two steps: lung segmentation and pulmonary nodule segmentation. For well-defined tasks such as pulmonary nodule segmentation on chest CT, automated machine learning tools are currently commercially available and have shown good performance in children [41]. Li et al. [41] achieved high accuracy (0.9479), Dice score (0.9678), precision (0.9711), and recall (0.9715) performance.

Tumor segmentations could be either automated or user guided. User-guided segmentation is more attainable but requires a dedicated viewer that supports AI algorithms and appropriate editing tools. Rickard et al. [42] described a semiautomatic segmentation algorithm for measuring tumor and kidney volumes on CT images of children with Wilms tumors before, during, and after treatment. This technique could potentially aid surgical planning, treatment response assessment, and prediction of long-term kidney function [42]. In 2023, deep learning–based AI algorithms have been used by Veiga-Canuto et al. [43], for neuroblastoma detection and segmentation on MRI, and by Klimont et al. [44], for automated segmentation and volumetry of pediatric lymphoma on contrast-enhanced CT.

Segmenting tumor lesions in whole-body imaging data presents unique challenges, particularly for pediatric patients. First, the high variability in imaging protocols across different institutions and scanners makes consistent lesion identification difficult. Second, the inherent complexity of multiorgan anatomy in whole-body images adds another layer of difficulty. Third, the diverse range of shapes and sizes in pediatric patients, spanning neonates to adolescents, further exacerbates these segmentation challenges. Deep learning–based tumor segmentation algorithms for whole-body CT, PET/CT, and MRI have been tested in adult patients with varying success [45, 46]. Deep learning algorithms for organ and lesion segmentation in adult patients can be cross-trained using transfer learning for applications in pediatric imaging. Figure 4 shows an example of U-Net–based segmentation algorithms, pretrained on adult CT and PET data and cross-trained for whole-body organ segmentation on CT and detection of tumor lesions on FDG PET.

Tumor Diagnosis and Treatment Response

Diagnosing tumors heavily relies on the ability of radiologists to assess multiple features such as location, size, border characteris-

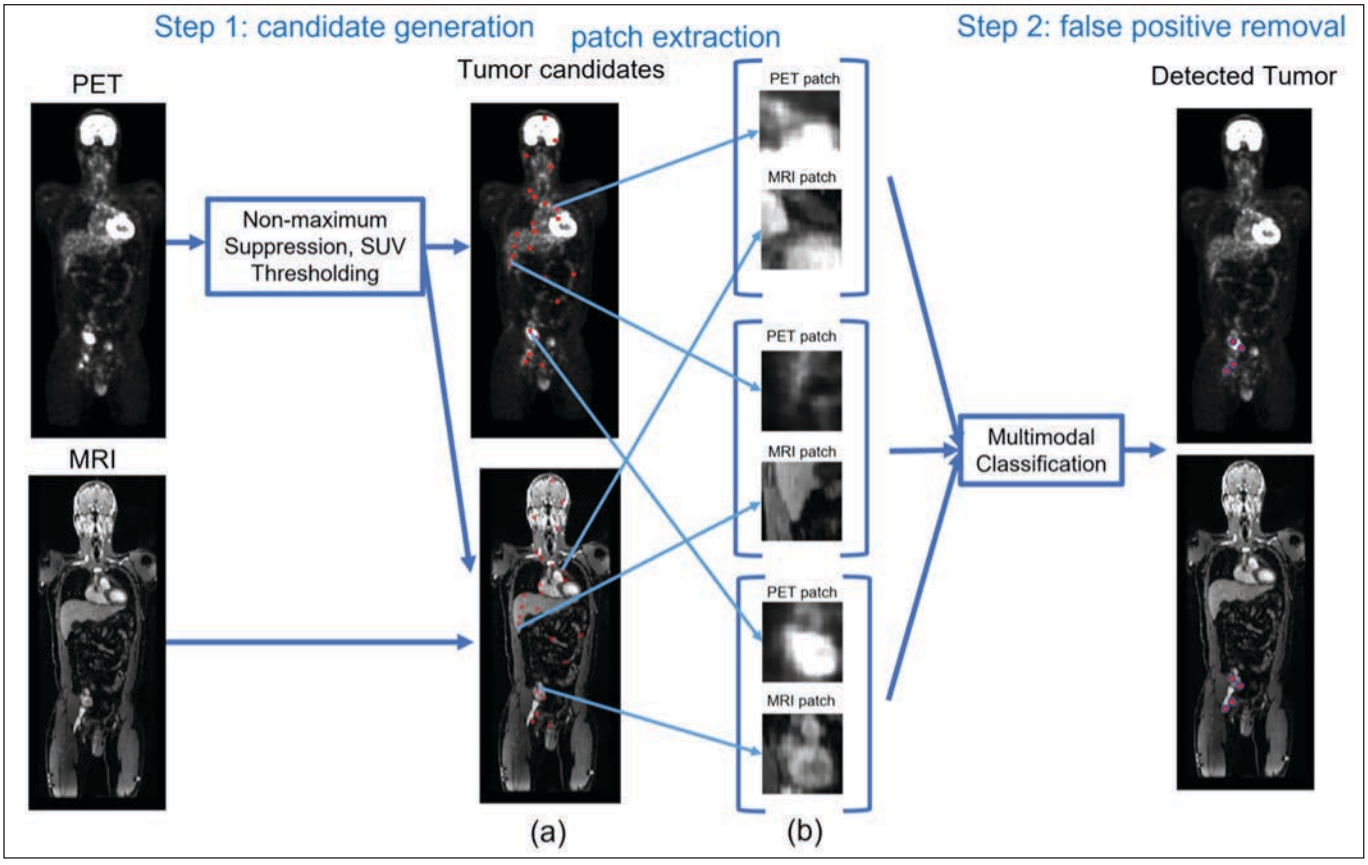

Fig. 5—Two-step method for detecting pediatric lymphoma. (Reproduced from [64], with permission)
A and **B**, Initially, potential tumor sites are identified by tumor candidate generation process using PET images, with nonmaximum suppression used to identify areas where SUV exceeds 2.0. Second step involves eliminating false-positive results. This process is achieved by use of deep learning–based algorithm and four experimental approaches that analyze patches extracted from both PET and MRI examinations through technique that integrates multiple imaging modalities.

tics, internal variation, and contrast material uptake. Researchers are actively developing AI and radiomic tools to assist radiologists in diagnosing pediatric tumors. Radiomics involves extracting and analyzing handcrafted mathematically defined image features, whereas AI encompasses a broader range of techniques, including deep learning methods, that may or may not use these features. Combining these approaches holds promise for improving patient care. However, limited pediatric data hinder the development and implementation of these tools in clinical settings.

Musculoskeletal Tumors

Osteosarcoma—Pereira et al. [47] built a machine learning–based radiomics model to predict lung metastases in patients with osteosarcoma using CT scans of the primary tumor. Their model, trained on data from 81 patients, achieved accuracy of 73% in identifying patients at risk for pulmonary metastases. Further validation on larger, diverse, and prospective datasets is needed to confirm the clinical utility of such approaches.

Teo et al. [48] developed a deep learning classification model for assessing the chemotherapy response of high-grade osteosarcoma on multimodal MRI in 10 children. They achieved an average accuracy of more than 90% in differentiating necrotic (dead) and viable tumor areas using conventional MR images such as T1-weighted, STIR, and postcontrast images. Diffusion-weighted MRI and dynamic contrast enhancement parameters further improved accuracy.

Huang et al. [49] compared different MRI techniques for assessing tumor response to chemotherapy in patients with osteosarcoma. Their machine learning model, which incorporated T1-, T2-, and diffusion-weighted MRI data, achieved higher accuracy than ADC alone in differentiating necrotic and viable tumor tissue.

Jeong et al. [50] investigated a machine learning approach using baseline FDG PET to predict response to neoadjuvant chemo-

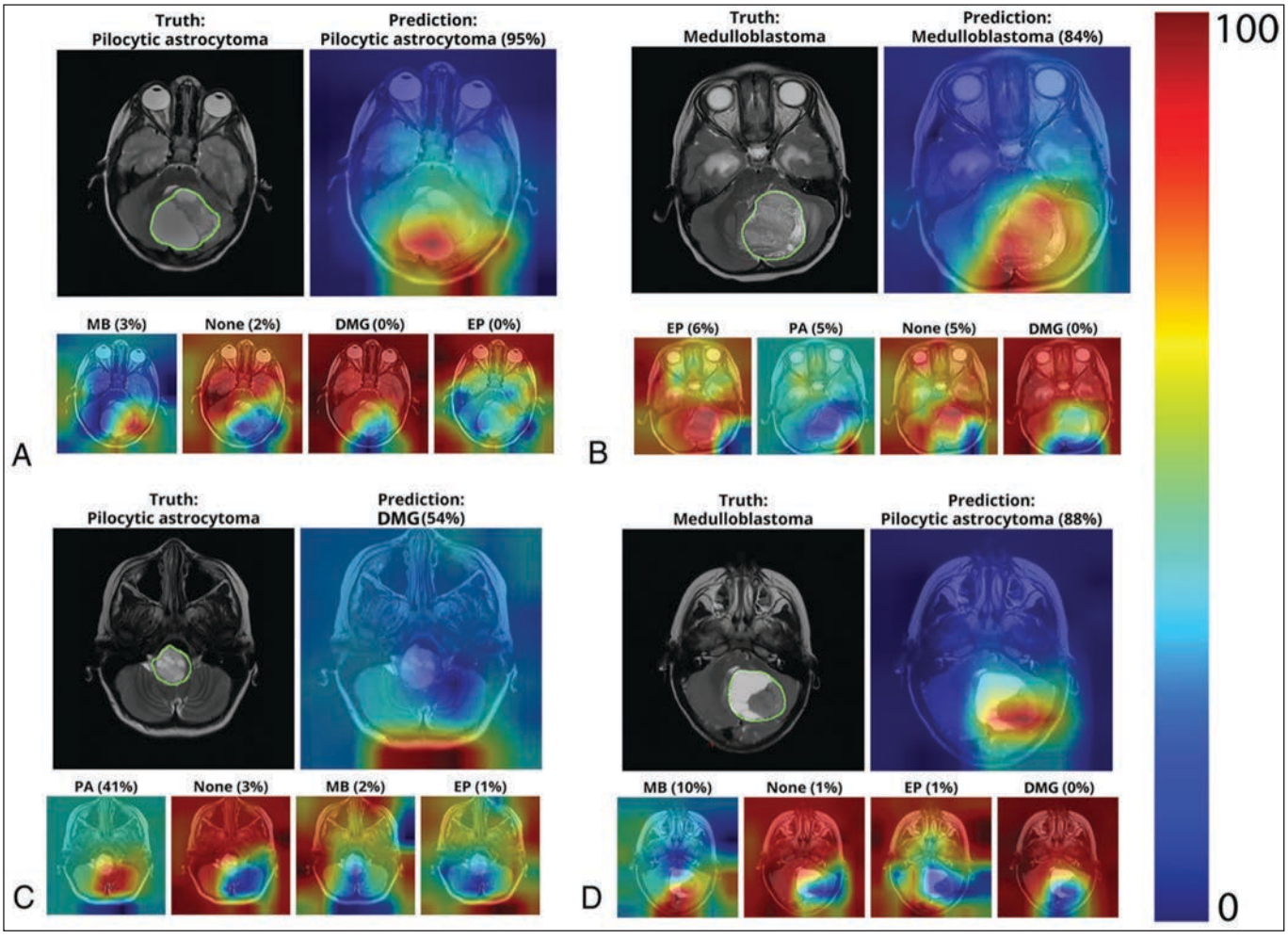

Fig. 6—Class activation maps produced by multiinstitutional MRI-based deep learning model developed by Quon et al. [6]. In each panel, top left image shows tumor areas manually outlined on T2-weighted image; top right image shows class activation map overlay of most-confident prediction made by model. Four images in bottom row show less-confident predictions. MB = medulloblastoma, DMG = diffuse midline glioma, EP = ependymoma, PA = pilocytic astrocytoma. (Used with permission of American Society of Neuroradiology, from Deep learning for pediatric posterior fossa tumor detection and classification: multiinstitutional study, Quon JL, Bala W, Chen LC, et al., *AJNR*, 41, 2020; permission conveyed through Copyright Clearance Center, Inc.)
A and **B,** Model correctly predicts PA (**A**) and MB (**B**).
C and **D,** Model incorrectly predicts DMG in patient with PA (**C**) and PA in patient with MB (**D**).

therapy in 70 patients with osteosarcoma. They analyzed both traditional PET metrics (SUV_{max} and tumor volume) and image-derived textural features. Although traditional metrics showed no significant difference between responders and nonresponders, machine learning models using textural features achieved better prediction accuracy (AUC up to 0.82). Analyzing the changes in FDG heterogeneity derived from PET using machine learning offered improved prediction accuracy (AUC up to 0.863). This study was limited by its small sample size. Consequently, the authors recommended a need for data from a larger patient cohort to validate the findings and develop a more robust predictive model.

Ewing sarcoma—Consalvo et al. [51] developed and validated an algorithm for the detection of bone tumors on 182 radiographs of 58 children. The algorithm achieved a diagnostic accuracy of 94.4% and 90.6% for lesion detection and 90.3% and 86.7% for the differentiation of osteomyelitis and Ewing sarcoma in validation and test data, respectively [51].

Gitto et al. [52] compared the predictive value of 3D and 2D MRI radiomics to assess response to neoadjuvant chemotherapy in 30 patients with Ewing sarcoma. The 3D radiomic feature model achieved sensitivity of 85% and specificity of 87% in predicting treatment response [52].

These results were not compared with those of human readers, who typically achieve sensitivities and specificities greater than 90% [53] given that Ewing sarcomas of bone usually show a significant decrease in size in response to chemotherapy [54, 55].

Abdominal Tumors

To date, limited research on the development of AI algorithms for the diagnosis of solid pediatric abdominal tumors on MRI and CT has been performed.

Wilms tumor—Zhu et al. [56] developed a CNN-based deep learning algorithm to differentiate 269 Wilms tumors from 95 non-Wilms tumors on the basis of the preoperative triphasic CT images of 364 pediatric patients, with histopathology used as the reference standard. AI achieved significantly higher sensitivity (78.1%) for identifying non-Wilms tumors than did the human experts (13.3–20%). Ma et al. [57] developed a support vector machine (SVM) model with 15 radiomic features to distinguish early- and advanced-stage Wilms tumors on preoperative CT in 118 children. The model showed accuracy, sensitivity, and specificity of 79%, 87%, and 69%, respectively [57]. Further development is needed to distinguish all four Wilms tumor stages (1–4) for more precise clinical guidance. This path reflects the incremental nature of AI development, whereby future work builds on initial successes.

In Europe, where preoperative chemotherapy for Wilms tumors is common, Sharaby et al. [58] developed a computer-aided system to predict treatment response in 63 patients with 46 chemotherapy-responsive and 17 nonresponsive Wilms tumors. Their model achieved accuracy of 95.24%, sensitivity of 95.65%, and specificity of 94.12% for prediction of chemotherapy response. That study did not mention the reference standard. Resectability involves many features beyond the size, shape, and texture of the primary tumor, such as tumor thrombus presence and extent, infiltration of adjacent structures, and tumor rupture.

Neuroblastoma—Liu et al. [59] compared the performance of six machine learning algorithms to predict clinical outcomes in patients with neuroblastoma based on CT. An artificial neural network performed well for most outcomes, such as mortality, presence of metastasis, and grade of neuroblastic differentiation (mean AUC, 0.79 ± 0.045 [SD], 0.83 ± 0.034, and 0.80 ± 0.047, respectively) [59].

Veiga-Canuto et al. [43] tested an AI algorithm (nnU-Net) for automatically detecting and outlining neuroblastomas on MRI in children with neuroblastoma. AI achieved a success rate of 94% for tumor segmentation and was significantly faster than human-derived manual segmentations (mean time, 7.9 vs 124 seconds) [43].

Chen et al. [60] developed a CT-based machine learning model to extract radiomic features that may be linked to prediction of *MYCN* oncogene amplification in pediatric neuroblastoma. Random forest, SVM, and logistic regression models achieved similar high AUCs (0.851–0.909), significantly outperforming the Bayes model (AUC, 0.729) [60]. Feng et al. [61] built three machine learning models to predict the mitosis-karyorrhexis index (linked with response to chemotherapy) based on the FDG PET/CT and clinical data of 102 children with neuroblastoma. Future studies could correlate the mitosis-karyorrhexis index with MIBG scans.

Pulmonary Nodules

For the detection of pulmonary nodules, some AI algorithms provide encouraging results [62], whereas others report inferior performance of algorithms trained on adult datasets for the detection of lung lesions on the chest radiographs [63] or CT scans [8, 9] of pediatric patients. Ni et al. [62] compared a deep CNN model (3087 detections and 278 misses) with the readings of junior physicians (2442 detections and 657 misses) for identifying pulmonary nodules in patients with osteosarcoma (109 nodules on 675 CT examinations). The deep CNN model achieved significantly higher sensitivity (92.3% vs 90.8%), specificity (55.2% vs 35.1%), and AUC (0.795 vs 0.687), indicating better detection and potentially greater accuracy. Additionally, the deep CNN model accelerated reading times compared with human interpretations. Shin et al. [63] used an adult-trained ResNet34 CNN for detection of lung lesions on 2273 pediatric chest radiographs and achieved an overall accuracy of only 87.5% (sensitivity, 67.2%; specificity, 91.1%). Exclusion of children younger than 2 years old and patients with cardiomegaly significantly improved the model's performance (accuracy, 96.9%; sensitivity, 86.4%; specificity, 97.9%). Hardie et al. [9] found that two CAD systems trained on adult data had lower sensitivity for detection of pulmonary nodules on chest CT in children (FlyerScan, 68.4%; Medical Open Network for Artificial Intelligence [MONAI], 53.1%) than in adults (FlyerScan, 83.9%; MONAI, 95.5%), highlighting the need for pediatric-specific training data for accurate diagnoses.

Lymphoma

Although substantial attempts have been made to develop AI algorithms for detecting lymphoma on FDG PET/CT in adults, few applications to date have focused on pediatric patients. Wang et al. [64] pioneered AI-based detection of pediatric lymphoma using FDG PET and T1-weighted MRI. Their two-stage approach (50 training and 20 testing datasets) focused on identifying regions of high radiotracer uptake on PET (likely representing tumors), followed by false-positive removal. A CNN-based multimodal fusion method incorporating PET and MRI data addressed these false-positives, highlighting AI's potential for this application [64] (Fig. 5).

Brain Tumors

AI has facilitated the diagnosis, segmentation, and detection of brain tumors [6, 65, 66]. In 2022, a systematic review reported that 22 studies on AI applications for pediatric brain tumor imaging identified tumor diagnosis as the dominant application, followed by tumor segmentation and detection [67]. Although five of six studies comparing AI to human experts favored AI for tumor diagnosis, none reported real-world clinical implementation of AI for this purpose [67].

Quon et al. [6] established a multiinstitutional MRI-based deep learning model for the detection and pathology classification of posterior fossa tumors in 600 pediatric patients. The model achieved an overall tumor detection and classification accuracy that was comparable with the performance of four board-certified radiologists [6] (Fig. 6).

Pisapia et al. [68] investigated an MRI-based machine learning model for predicting progression of optic pathway gliomas (OPGs). The model, trained on data from 19 progressing and 19 nonprogressing tumors, incorporated manual segmentation of optic nerves and diffusion tractography for optic radiations. Analyzing features derived from various MRI sequences, including diffusion tensor imaging (DTI), the model achieved high accuracy (86%), sensitivity (89%), and specificity (81%) for the prediction of OPG progression. A key predictive feature was the fractional anisotropy of the optic radiations on DTI (AUC, 0.83).

Zhou et al. [65] developed an automatic machine learning model based on MRI in 288 patients with posterior fossa tumors. A radiomic model of automatic machine learning with the tree-based pipeline optimization tool (TPOT) outperformed expert radiologists [65].

Conclusion and Future Directions

Machine learning algorithms hold promise for pediatric oncology imaging, offering faster, cheaper, and potentially safer medical imaging methods for children with cancer. Challenges include the relative scarcity of pediatric cancer imaging data, inhomogeneity of multiinstitutional datasets, data distribution shifts, and lack of commercially available AI tools for pediatric imaging applications. Additional impediments to clinical translation include the diverse anatomies of growing children and the presence of nonstandardized imaging protocols.

Possible solutions include standardized imaging protocols, improved data harmonization techniques, formation of multiinstitutional consortia for data sharing, and generation of data repositories for transfer learning from datasets that include adult and pediatric cases. Increased efforts such as those of The Cancer Imaging Archive, the Children's Oncology Group, and the CBTN are required to ensure that data availability will not be a major hurdle for developing AI algorithms. AI algorithms trained on adult data alone may not perform well on children due to anatomic and physiologic differences, highlighting the need for transfer learning and the generation of pediatric-specific models. The initial results from machine learning–based radiomics models are encouraging, but prospective validation is necessary to ensure generalizability and real-world effectiveness. Additional opportunities include leveraging reconstruction algorithms to achieve accelerated low-dose imaging and automating the generation of metric-based staging and treatment monitoring scores.

Despite current limitations, AI offers a compelling path forward for pediatric oncology imaging. In contrast to human experts, who have a limited learning period and eventually retire, AI models hold the promise of perpetual learning. This continuous improvement across vast datasets, spanning generations of human expertise, can lead to significant performance gains over decades to come. As AI integration in clinical practice accelerates, robust safeguards are essential to ensure continued clinician autonomy in the event of system downtime. Transfer learning of adult-based AI models to pediatric cancers, multiinstitutional data sharing, and ethical data privacy practices for pediatric patients with rare cancers will be keys to achieving robust validation and unlocking AI's full potential for clinical translation and improved outcomes for these young patients.

Provenance and review: Not solicited; externally peer reviewed.

Peer reviewers: Ashishkumar K. Parikh, Children's Healthcare of Atlanta/Emory University; additional individual(s) who chose not to disclose their identity.

References

1. Wang YJ, Baratto L, Hawk KE, et al. Artificial intelligence enables whole-body positron emission tomography scans with minimal radiation exposure. *Eur J Nucl Med Mol Imaging* 2021; 48:2771–2781
2. Theruvath AJ, Siedek F, Yerneni K, et al. Validation of deep learning-based augmentation for reduced ^{18}F-FDG dose for PET/MRI in children and young adults with lymphoma. *Radiol Artif Intell* 2021; 3:e200232
3. Chaudhari AS, Mittra E, Davidzon GA, et al. Low-count whole-body PET with deep learning in a multicenter and externally validated study. *NPJ Digit Med* 2021; 4:127
4. Lavdas I, Glocker B, Kamnitsas K, et al. Fully automatic, multiorgan segmentation in normal whole body magnetic resonance imaging (MRI), using classification forests (CFs), convolutional neural networks (CNNs), and a multi-atlas (MA) approach. *Med Phys* 2017; 44:5210–5220
5. Bianconi F, Fravolini ML, Pizzoli S, et al. Comparative evaluation of conventional and deep learning methods for semi-automated segmentation of pulmonary nodules on CT. *Quant Imaging Med Surg* 2021; 11:3286–3305
6. Quon JL, Bala W, Chen LC, et al. Deep learning for pediatric posterior fossa tumor detection and classification: a multi-institutional study. *AJNR* 2020; 41:1718–1725
7. American College of Radiology Data Science Institute website. AI central. aicentral.acrdsi.org. Accessed Aug 9, 2023
8. Salman R, Nguyen HN, Sher AC, Hallam KA, Seghers VJ, Sammer MBK. Diagnostic performance of artificial intelligence for pediatric pulmonary nodule detection in computed tomography of the chest. *Clin Imaging* 2023; 101:50–55
9. Hardie RC, Trout AT, Dillman JR, Narayanan BN, Tanimoto AA. Performance analysis in children of traditional and deep learning CT lung nodule computer-aided detection systems trained on adults. *AJR* 2024; 222:e2330345
10. NIH National Cancer Institute Cancer Imaging Program website. Cancer Imaging Archive: pediatric data collections and analysis. www.cancerimagingarchive.net/pediatric-data-collections-and-analysis. Accessed Mar 19, 2024
11. Medical Imaging and Data Resource Center (MIDRC) website. MIDRC. www.midrc.org/. Accessed Feb 7, 2024
12. Halabi SS, Prevedello LM, Kalpathy-Cramer J, et al. The RSNA pediatric bone age machine learning challenge. *Radiology* 2019; 290:498–503
13. Children's Oncology Group website. COG registry: project—every child. childrensoncologygroup.org/cog-registry-project-everychild. Accessed Mar 19, 2024

14. Familiar AM, Kazerooni AF, Anderson H, et al. A multi-institutional pediatric dataset of clinical radiology MRIs by the Children's Brain Tumor Network. ArXiv website. arxiv.org/pdf/2310.01413. Published Oct 2, 2023. Accessed Mar 15, 2024
15. Brady SL, Yee BS, Kaufman RA. Characterization of adaptive statistical iterative reconstruction algorithm for dose reduction in CT: a pediatric oncology perspective. *Med Phys* 2012; 39:5520–5531
16. Lin DJ, Walter SS, Fritz J. Artificial intelligence-driven ultra-fast superresolution MRI: 10-fold accelerated musculoskeletal turbo spin echo MRI within reach. *Invest Radiol* 2023; 58:28–42
17. Akai H, Yasaka K, Sugawara H, et al. Commercially available deep-learning-reconstruction of MR imaging of the knee at 1.5T has higher image quality than conventionally-reconstructed imaging at 3T: a normal volunteer study. *Magn Reson Med Sci* 2023; 22:353–360
18. Canon Medical Systems website. MRI: deep learning reconstruction. us.medical.canon/products/magnetic-resonance/aice/dlr. Accessed Apr 12, 2024
19. Wang YJ, Wang P, Adams LC, et al. Low-count whole-body PET/MRI restoration: an evaluation of dose reduction spectrum and five state-of-the-art artificial intelligence models. *Eur J Nucl Med Mol Imaging* 2023; 50:1337–1350
20. Ladefoged CN, Marner L, Hindsholm A, Law I, Højgaard L, Andersen FL. Deep learning based attenuation correction of PET/MRI in pediatric brain tumor patients: evaluation in a clinical setting. *Front Neurosci* 2019; 12:1005
21. Maspero M, Bentvelzen LG, Savenije MHF, et al. Deep learning-based synthetic CT generation for paediatric brain MR-only photon and proton radiotherapy. *Radiother Oncol* 2020; 153:197–204
22. Ma JJ, Nakarmi U, Kin CYS, et al. Diagnostic image quality assessment and classification in medical imaging: opportunities and challenges. In: *2020 IEEE 17th International Symposium on Biomedical Imaging (ISBI)*. IEEE, 2020:337–340
23. Lee HK, Song JS, Jang W, Nickel D, Paek MY. Improved single breath-hold SSFSE sequence for liver MRI based on compressed sensing: evaluation of image quality compared with conventional T2-weighted sequences. *Diagnostics (Basel)* 2022; 12:2164
24. Salman R, Nguyen HN, Sher AC, Hallam K, Seghers VJ, Sammer MBK. Diagnostic performance of artificial intelligence for pediatric pulmonary nodule detection on chest computed tomography: comparison of simulated lower radiation doses. *Eur J Pediatr* 2023; 182:5159–5165
25. Desai AD, Ozturkler BM, Sandino CM, et al. Noise2Recon: enabling SNR-robust MRI reconstruction with semi-supervised and self-supervised learning. *Magn Reson Med* 2023; 90:2052–2070
26. Ronneberger O, Fischer P, Brox T. U-Net: convolutional networks for biomedical image segmentation. In: Navib N, Hornegger J, Wells WM, Frangi AF, eds. *Medical image computing and computer-assisted intervention: MICCAI 2015*. Springer International, 2015:234–241
27. Isensee F, Jaeger PF, Kohl SAA, Petersen J, Maier-Hein KH. nnU-Net: a self-configuring method for deep learning-based biomedical image segmentation. *Nat Methods* 2021; 18:203–211
28. Kart T, Fischer M, Küstner T, et al. Deep learning-based automated abdominal organ segmentation in the UK Biobank and German National Cohort magnetic resonance imaging studies. *Invest Radiol* 2021; 56:401–408
29. Antonelli M, Reinke A, Bakas S, et al. The medical segmentation decathlon. *Nat Commun* 2022; 13:4128
30. Karimi-Bidhendi S, Arafati A, Cheng AL, Wu Y, Kheradvar A, Jafarkhani H. Fully automated deep learning segmentation of pediatric cardiovascular magnetic resonance of patients with complex congenital heart diseases. *J Cardiovasc Magn Reson* 2020; 22:80
31. Kazerooni AF, Arif S, Madhogarhia R, et al. Automated tumor segmentation and brain tissue extraction from multiparametric MRI of pediatric brain tumors: a multi-institutional study. medRxiv website. www.medrxiv.org/content/10.1101/2023.01.02.22284037v1. Published Jan 11, 2023. Accessed Jul 18, 2023
32. Jordan P, Adamson PM, Bhattbhatt V, et al. Pediatric chest-abdomen-pelvis and abdomen-pelvis CT images with expert organ contours. *Med Phys* 2022; 49:3523–3528
33. Rister B, Yi D, Shivakumar K, Nobashi T, Rubin DL. CT-ORG, a new dataset for multiple organ segmentation in computed tomography. *Sci Data* 2020; 7:381
34. Kofler F, Berger C, Waldmannstetter D, et al. BraTS toolkit: translating BraTS brain tumor segmentation algorithms into clinical and scientific practice. *Front Neurosci* 2020; 14:125
35. Peng J, Kim DD, Patel JB, et al. Deep learning-based automatic tumor burden assessment of pediatric high-grade gliomas, medulloblastomas, and other leptomeningeal seeding tumors. *Neuro Oncol* 2022; 24:289–299
36. Kazerooni AF, Khalili N, Liu X, et al. The brain tumor segmentation (BraTS) challenge 2023: focus on pediatrics (CBTN-CONNECT-DIPGR-ASNR-MICCAI BraTS-PEDs). ArXiv website. arxiv.org/abs/2305.17033. Published Jul 7, 2023. Accessed Jul 18, 2023
37. Moawad AW, Janas A, Baid U, et al. The brain tumor segmentation (BraTS-METS) challenge 2023: brain metastasis segmentation on pre-treatment MRI. ArXiv website. arxiv.org/abs/2306.00838. Published Jun 1, 2023. Accessed Jul 18, 2023
38. Drai M, Testud B, Brun G, et al. Borrowing strength from adults: transferability of AI algorithms for paediatric brain and tumour segmentation. *Eur J Radiol* 2022; 151:110291
39. Fathi Kazerooni A, Arif S, Madhogarhia R, et al. Automated tumor segmentation and brain tissue extraction from multiparametric MRI of pediatric brain tumors: a multi-institutional study. *Neurooncol Adv* 2023; 5:vdad027
40. Ladefoged CN, Henriksen OM, Mathiasen R, et al. Automatic detection and delineation of pediatric gliomas on combined [^{18}F]FET PET and MRI. *Front Nucl Med* 2022 Aug 24 [published online]
41. Li Z, Yang L, Shu L, et al. Research on CT lung segmentation method of preschool children based on traditional image processing and ResUnet. *Comput Math Methods Med* 2022; 2022:7321330
42. Rickard M, Fernandez N, Blais AS, et al. Volumetric assessment of unaffected parenchyma and Wilms' tumours: analysis of response to chemotherapy and surgery using a semi-automated segmentation algorithm in children with renal neoplasms. *BJU Int* 2020; 125:695–701
43. Veiga-Canuto D, Cerdà-Alberich L, Jiménez-Pastor A, et al. Independent validation of a deep learning nnU-Net tool for neuroblastoma detection and segmentation in MR images. *Cancers (Basel)* 2023; 15:1622
44. Klimont M, Oronowicz-Jaśkowiak A, Flieger M, Rzeszutek J, Juszkat R, Jończyk-Potoczna K. Deep learning-based segmentation and volume calculation of pediatric lymphoma on contrast-enhanced computed tomographies. *J Pers Med* 2023; 13:184
45. Hering A, Peisen F, Amaral T, et al. Whole-body soft-tissue lesion tracking and segmentation in longitudinal CT imaging studies. *Proc Mach Learn Res* 2021; 243:312–326
46. Gatidis S, Hepp T, Früh M, et al. A whole-body FDG-PET/CT dataset with manually annotated tumor lesions. *Sci Data* 2022; 9:601
47. Pereira HM, Leite Duarte ME, Ribeiro Damasceno I, de Oliveira Moura Santos LA, Nogueira-Barbosa MH. Machine learning-based CT radiomics features for the prediction of pulmonary metastasis in osteosarcoma. *Br J Radiol* 2021; 94:20201391
48. Teo KY, Daescu O, Cederberg K, Sengupta A, Leavey PJ. Correlation of histopathology and multi-modal magnetic resonance imaging in childhood osteosarcoma: predicting tumor response to chemotherapy. *PLoS One* 2022; 17:e0259564

49. Huang B, Wang J, Sun M, et al. Feasibility of multi-parametric magnetic resonance imaging combined with machine learning in the assessment of necrosis of osteosarcoma after neoadjuvant chemotherapy: a preliminary study. *BMC Cancer* 2020; 20:322
50. Jeong SY, Kim W, Byun BH, et al. Prediction of chemotherapy response of osteosarcoma using baseline ^{18}F-FDG textural features machine learning approaches with PCA. *Contrast Media Mol Imaging* 2019; 2019:3515080
51. Consalvo S, Hinterwimmer F, Neumann J, et al. Two-phase deep learning algorithm for detection and differentiation of Ewing sarcoma and acute osteomyelitis in paediatric radiographs. *Anticancer Res* 2022; 42:4371–4380
52. Gitto S, Corino VDA, Annovazzi A, et al. 3D vs. 2D MRI radiomics in skeletal Ewing sarcoma: feature reproducibility and preliminary machine learning analysis on neoadjuvant chemotherapy response prediction. *Front Oncol* 2022; 12:1016123
53. Bosma SE, Vriens D, Gelderblom H, van de Sande MAJ, Dijkstra PDS, Bloem JL. ^{18}F-FDG PET-CT versus MRI for detection of skeletal metastasis in Ewing sarcoma. *Skeletal Radiol* 2019; 48:1735–1746
54. Aghighi M, Boe J, Rosenberg J, et al. Three-dimensional radiologic assessment of chemotherapy response in Ewing sarcoma can be used to predict clinical outcome. *Radiology* 2016; 280:905–915
55. Olmos D, Postel-Vinay S, Molife LR, et al. Safety, pharmacokinetics, and preliminary activity of the anti-IGF-1R antibody figitumumab (CP-751,871) in patients with sarcoma and Ewing's sarcoma: a phase 1 expansion cohort study. *Lancet Oncol* 2010; 11:129–135
56. Zhu Y, Li H, Huang Y, et al. CT-based identification of pediatric non-Wilms tumors using convolutional neural networks at a single center. *Pediatr Res* 2023; 94:1104–1110
57. Ma XH, Shu L, Jia X, et al. Machine learning-based CT radiomics method for identifying the stage of Wilms tumor in children. *Front Pediatr* 2022; 10:873035
58. Sharaby I, Alksas A, Nashat A, et al. Prediction of Wilms' tumor susceptibility to preoperative chemotherapy using a novel computer-aided prediction system. *Diagnostics (Basel)* 2023; 13:486
59. Liu G, Poon M, Zapala MA, et al. Incorporating radiomics into machine learning models to predict outcomes of neuroblastoma. *J Digit Imaging* 2022; 35:605–612
60. Chen X, Wang H, Huang K, et al. CT-based radiomics signature with machine learning predicts MYCN amplification in pediatric abdominal neuroblastoma. *Front Oncol* 2021; 11:687884
61. Feng L, Qian L, Yang S, et al. Prediction for mitosis-karyorrhexis index status of pediatric neuroblastoma via machine learning based ^{18}F-FDG PET/CT radiomics. *Diagnostics (Basel)* 2022; 12:262
62. Ni YL, Zheng XC, Shi XJ, Xu YF, Li H. Deep convolutional neural network based on CT images of pulmonary nodules in the lungs of adolescent and young adult patients with osteosarcoma. *Oncol Lett* 2023; 26:344
63. Shin HJ, Son NH, Kim MJ, Kim EK. Diagnostic performance of artificial intelligence approved for adults for the interpretation of pediatric chest radiographs. *Sci Rep* 2022; 12:10215
64. Wang H, Sarrami A, Wu JTY, et al. Multimodal pediatric lymphoma detection using PET and MRI. *AMIA Annu Symp Proc* 2024; 2023:736–743
65. Zhou H, Hu R, Tang O, et al. Automatic machine learning to differentiate pediatric posterior fossa tumors on routine MR imaging. *AJNR* 2020; 41:1279–1285
66. Zhang M, Tam L, Wright J, et al. Radiomics can distinguish pediatric supratentorial embryonal tumors, high-grade gliomas, and ependymomas. *AJNR* 2022; 43:603–610
67. Huang J, Shlobin NA, Lam SK, DeCuypere M. Artificial intelligence applications in pediatric brain tumor imaging: a systematic review. *World Neurosurg* 2022; 157:99–105
68. Pisapia JM, Akbari H, Rozycki M, et al. Predicting pediatric optic pathway glioma progression using advanced magnetic resonance image analysis and machine learning. *Neurooncol Adv* 2020; 2:vdaa090
69. Shiyam Sundar LK, Yu J, Muzik O, et al. Fully automated, semantic segmentation of whole-body ^{18}F-FDG PET/CT images based on data-centric artificial intelligence. *J Nucl Med* 2022; 63:1941–1948

(Editorial Comment starts on next page)

Editorial Comment: The Radiologist's Role in Artificial Intelligence for Pediatric Oncologic Imaging

Artificial intelligence (AI) is growing at an exponential pace and impacting our lives in myriad ways. From planning the most efficient morning commute to providing book recommendations for leisure reading, AI is designed to augment many of our experiences in the world. As radiologists, we have an opportunity to incorporate elements from the burgeoning AI revolution into the imaging-based care we provide for our patients.

Much like AI's application in our personal lives, the arc of radiology's potential AI application is broad. This article nicely summarizes the many roles AI may have in imaging pediatric patients with cancer [1]. Although some applications, such as AI-aided image reconstruction, are today's realities, other applications, such as imaging-based outcomes prognostication for children with cancer, are concepts we hope to see in practice in the not-too-distant future.

The road to achieving AI's full potential for application in pediatric oncologic imaging will not be without obstacles. Prior articles have discussed the unique impediments to progress in AI development for pediatric patients, yielding a dearth of FDA-approved algorithms and a health equity deficit for this vulnerable population [2, 3].

While reading this review article, I hope you ask: "What is my role in bringing AI to imaging care for pediatric patients?" There are many possible answers, but I believe two important ones are to be curious (i.e., stay informed about relevant AI technology and critically appraise how its application may allow improved care for your patients) and be an advocate (i.e., encourage and, where feasible, participate in the development of safe, effective, and accessible AI tools designed and developed for pediatric patients).

AI holds the promise of an exciting future in the care of pediatric patients with cancer—one where we as radiologists remain integral members of a health care team that offers efficient, effective, precise, and personalized care.

Gary R. Schooler, MD
UT Southwestern Medical Center
Dallas, TX
Address correspondence to *gary.schooler@utsouthwestern.edu, @gschoolermd*

First published online: Jun 12, 2024 ▪ Version of record: Aug 14, 2024

The author declares that there are no disclosures relevant to the subject matter of this article.

doi.org/10.2214/AJR.24.31555 ▪ *AJR* 2024; 223:e2431555

ISSN-L 0361-803X/24/2232–e2431555 ▪ © American Roentgen Ray Society

Provenance and review: Solicited; not externally peer reviewed.

References

1. Singh SB, Sarrami AH, Gatidis S, Varniab ZS, Chaudhari A, Daldrup-Link HE. Applications of artificial intelligence for pediatric cancer imaging. *AJR* 2024; 223:e2431076
2. Sammer MBK, Akbari YS, Barth RA, et al. Use of artificial intelligence in radiology: impact on pediatric patients, a white paper from the ACR Pediatric AI Workgroup. *J Am Coll Radiol* 2023; 20:730–737
3. Sammer MBK, Sher AC, Towbin AJ. Ensuring adequate development and appropriate use of artificial intelligence in pediatric medical imaging. *AJR* 2022; 218:182–183